Journal of Magnetics 13(4), 136-139 (2008)

Numerical Formula of Depinning Fields from Notches in Ferromagnetic Permalloy Nanowire

Kab-Jin Kim[1], Chun-Yeol You[2], and Sug-Bong Choe[1]*

[1]*Center for Subwavelength Optics and School of Physics, Seoul National University, Seoul 151-742, Korea*
[2]*Department of Physics, Inha University, Incheon 402-751, Korea*

(Received 9 October 2008, Received in final form 24 November 2008, Accepted 25 November 2008)

A simplified equation of depinning fields from notches of ferromagnetic Permalloy nanowires is presented. The derived equation is given in the form of an explicit function of nanowire width and thickness, and notch depth and angle. The equation agrees with all micromagnetic simulation results to an accuracy of ± 0.5 mT.

Keywords : ferromagnetic nanowire, domain wall, notch, pinning

1. Introduction

In recent years, various novel architectures of ferromagnetic nanowires have been proposed for magnetic memory and logic devices [1, 2]. In these devices, data are stored in the form of magnetic domains which are partitioned by magnetic domain walls (DW). To control DW position precisely and stably it was proposed that structural defects, such as, notches, be placed on nanowires [3-7]. In general, a larger notch provides better stability against thermal fluctuations, but it requires a larger magnetic field and/or spin current to trigger DW motion [7]. Thus, the design of notches with optimized stability and controllability is a critical issue. In this paper, we present a phenomenological equation that predicts depinning fields quantitatively from notches in Permalloy nanowires.

2. Simulation Method

In the present study, we designed a model structure for nanowires. The length of nanowires was fixed to 10 times greater than wire width, and ends were tapered, as shown in Fig. 1(a). Longer wires better minimized the effects of stray field from wire ends. We confirmed that the stray field in our geometry had a negligible effect on depinning fields (less than 0.2 mT), by comparing stray fields of wires that were twice as long. A notch was placed at the center of a wire in the form of an equilateral triangle with the incline length l and an angle α, as shown in Fig. 1(b). Soft-magnetic Permalloy was chosen as a nanowire material, as has been previously described [4-12]. Saturation magnetization M_S in our simulations was 8.6×10^5 A/m and exchange stiffness A_X was 1.3×10^{-11} J/m.

Micromagnetic calculations were performed using OOMMF [13]. Simulations were carried out using the following steps. A transverse DW [14] was first located at the notch. A typical DW configuration is illustrated in Fig. 1(a), in which the gray contrast corresponds to the y component of the magnetization. The arrows indicate the magnetization direction and the dotted lines guide the triangular shape of the transverse DW. In this study, we focused on the transverse DW rather than vortex DW, since the former appears thinner and narrower so that required for practical applications [15]. Vortex DW formation was excluded by our initial conditions. An external magnetic field was then applied along +x direction to trigger the DW motion. The equilibrium state was attained for all magnetic fields with increments of 0.1 mT. An internal maximum torque of

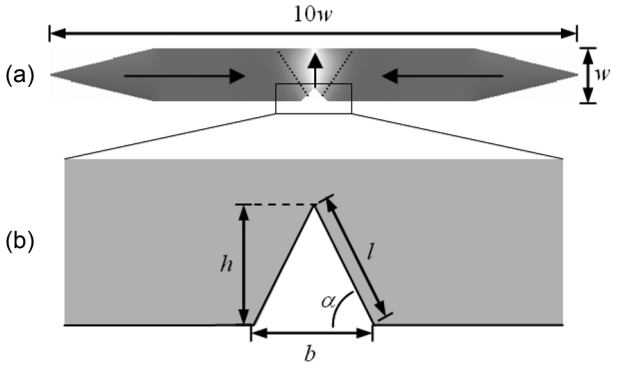

Fig. 1. Geometry of the (a) nanowire and (b) notch used in the simulation.

*Corresponding author: Tel: +82-2-880-9254
Fax: +82-2-884-9254, e-mail: sugbong@snu.ac.kr

$<2\times10^{-4}\ M_S^2$ was employed as the criterion of equilibrium. A relatively large Gilbert damping parameter (0.5) was used for fast relaxation. Above a certain field strength the DW escaped from the notch, followed by saturation of the wire in the field direction. We denote this critical field as the depinning field H_{dp}. Depinning fields were evaluated with respect to wire width and thickness and notch size and angle. The cell size was chosen to be 2.5 nm, which was sufficiently smaller than the exchange length (~5.3 nm), in order to elaborate the notch.

3. Results and Discussion

Fig. 2(a) shows calculated depinning fields with respect to notch sizes for several widths of nanowires. The figure shows that depinning fields converged with increasing notch size. This convergent behavior originates from dynamic narrowing of the DW width under an applied magnetic field. Fig. 3 shows snapshots of DW configurations at the instant of depinning for (a) 40 nm and (b) 80 nm deep notches. The external magnetic field pushed the DW to the right to reduce Zeeman energy. With increasing magnetic field strength, the upper end position Q of the DW center moves up to the upper end of the wire and the lower end position P moves down to the right incline of the notch, as

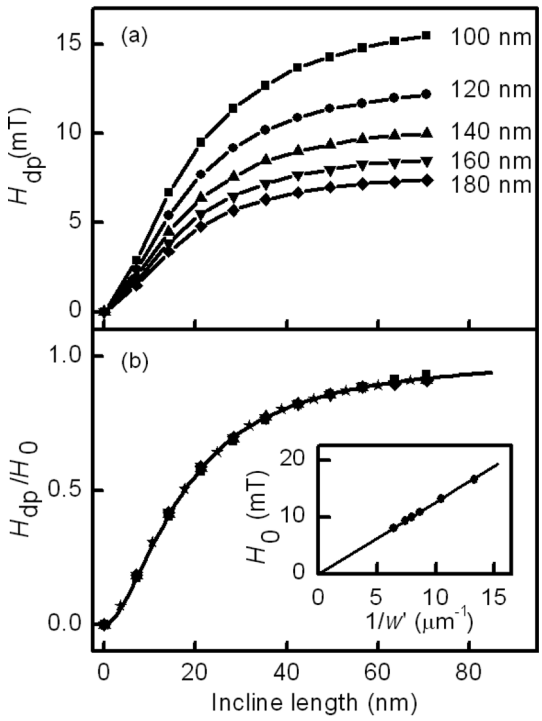

Fig. 2. (a) Depinning field with respect to notch incline length for several different nanowire widths as denoted in the figure. Film thickness and notch angle were fixed at t=5 nm and $\alpha=\pi/4$. (b) Normalized depinning field. The solid line was best fitted by Eq. (2). Inset: The saturation value H_0 vs. the inverse of w'. The solid line was best fitted by Eq. (3).

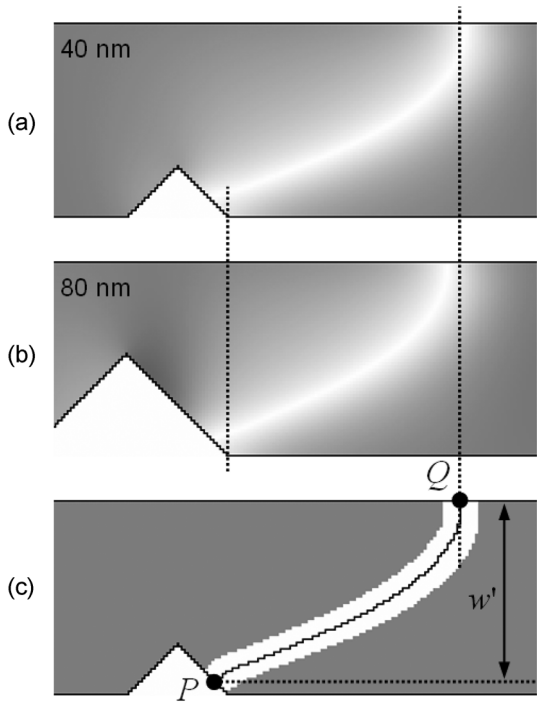

Fig. 3. Snapshots taken at the moment of depinning for (a) 40 nm and (b) 80 nm deep notches. (c) A sketch of the DW configuration.

illustrated in Fig. 3(c). At depinning field, P reaches the bottom right vertex, and finally, it escapes from the notch. Note that the DW narrowed to a certain finite width. It was interesting to observe that the two snapshots were almost identical irrespective of notch size, which was ascribed to the finite width of the DW. Due to its finite width, short-range exchange interactions from the DW were exerted only on the right side of the notch and dipolar coupling with the left side diminished with increasing notch size.

DW width l_{DW} was estimated to be 70 nm for the condition $M_x^2 < \frac{1}{2}M_S^2$ inside the wall. Due to the finite DW width, the lowest position P before depinning was $\frac{1}{2}l_{dw}$ away from the right vertex, and the distance between P and the upper edge of the wire was given by

$$w' = (w - \tfrac{1}{2} l_{dw} \sin\alpha), \tag{1}$$

as denoted in Fig. 3(c). It plays an important role as a scaling parameter for determining depinning fields, as discussed later.

Interestingly, there appears to be a universal law for depinning fields. By normalizing the curves in Fig. 2(a) with their saturation values, all curves tended to a unique curve. This universal curve is shown in Fig. 2(b), and is excellently fitted by:

$$\frac{H_{dp}}{H_0} = f(l), \text{ with } f(l) = \frac{1}{1 + (\frac{1}{4} l_{dw}/l)^{7/4}}. \tag{2}$$

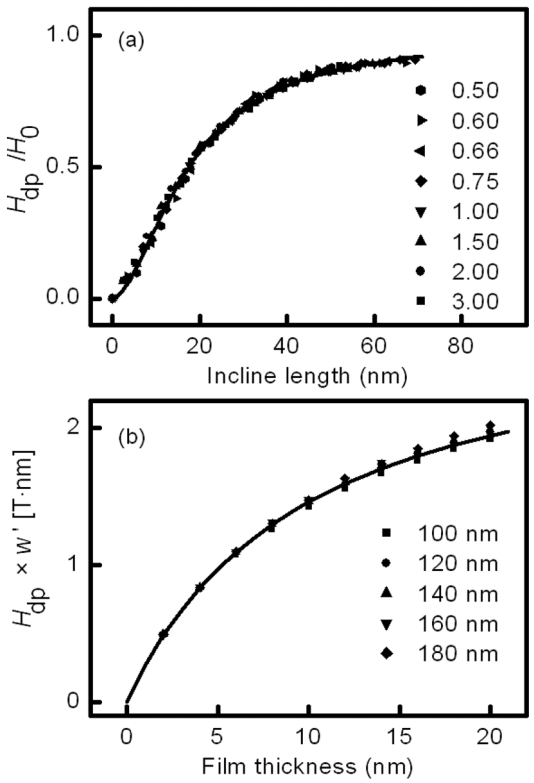

Fig. 4. (a) Normalized depinning field for several notch angles. The numbers denoted are tanα values. Film thickness and notch angle were fixed to t=5 nm and w=150 nm. The solid line was bested fitted by Eq. (2). (b) Normalized depinning field for several different nanowire widths. The notch size and angle were fixed to l=25 nm and $\alpha=\pi/4$. The solid line was bested fitted by Eq. (5).

The saturation value H_0 was found to be simply proportional to the inverse of w', irrespective of microscopic details. The inset in Fig. 2(b) shows the saturation field H_0 with respect to the inverse of w', and the solid line displays the best proportional fit i.e.

$$H_0=\frac{\gamma}{w'}, \text{ with } \gamma=1.26 \text{ [T·nm]}. \tag{3}$$

The universality was valid for various notch angles α. Fig. 4(a) shows the normalized depinning field for several different angles. It was surprising to find that all values fitted a single unique curve. The unique curve also fit Eq. (2), as shown by the solid line in Fig. 4(a). The saturation value again shows an inverse relation between w' and the additional correction factor $g(\alpha)$ i.e.,

$$\gamma \rightarrow \gamma \times g\left(\frac{\alpha}{\alpha_0}\right), \text{ with } g(x)=x(1.834-0.87x+0.36x^3), \tag{4}$$

where $\alpha_0=\pi/4$. The enhancement of H_{dp} with increasing α can be readily expected. However, H_{dp} decreases at large α. This decrement is caused by the dipolar interaction between the two sides of the notch due to narrow and sharp separation. Maximum H_{dp} was attained at an angle of *ca.* $\pi/3$ radian (60°).

Finally, film thickness dependence was examined. Depinning fields were evaluated by changing the film thicknesses for several wire widths. The effect of different wire widths could be removed by plotting $\gamma(=w'H_{dp}/f(l))$ with respect to film thickness. Once again, all values fell onto the unique curve as shown in Fig. 4(b). This curve was fitted by the function

$$\gamma \rightarrow \gamma(t), \text{ with } \gamma(t)=\gamma_0\frac{t}{t+t_0} \tag{5}$$

where γ_0=3.78[T·nm] and t_0=10 nm.

We finalize the phenomenological equation of the depinning field by combining Eqs. (1)-(5). The final equation then became

$$H_{dp}=\frac{\gamma_0}{w-\frac{1}{2}l_{dw}\sin\alpha}\cdot\frac{t}{t+t_0}\cdot\frac{g(\alpha)}{1+(\frac{1}{4}l_{dw}/l)^{7/4}}. \tag{6}$$

All simulation results presented here fitted Eq. (6) within a maximum error of ±0.5 mT. Maximum deviations were observed for thicker films or smaller notches. The former might be ascribed to the deformation to the asymmetric transverse wall in thick films and the latter to the finite cell size in the simulation. Other than these cases, most values agreed within ±0.2 mT, which is much less than the deviation from structural irregularity. For reference, a 2-nm inaccuracy in notch size resulted in a *ca.* ±0.8 mT change in the depinning field of small notches.

4. Conclusions

We examined the depinning mechanism for notches in Permalloy nanowires. Domain-wall width was found to be the important parameter for geometric scaling, and notch incline length rather than notch depth determined depinning fields. A phenomenological equation for the depinning field from Permalloy nanowire is presented as a function of the wire width, thickness, notch size, and angle. The derived equation agreed with all simulation results within a maximum error of ±0.5 mT.

Acknowledgment

This work was supported by a Korean Research Foundation Grant funded by the Korean Government (MOEHRD) (KRF-2006-312-C00529).

References

[1] L. Thomas, M. Hayashi, X. Jiang, R. Moriya, C. Rettner, and S. S. P, Parkin, Nature **443**, 197 (2006).

[2] D. A. Allwood, G. Xiong, C. Faulkner, D. Atkinson, D. Petit, and R. P, Cowburn, Science **309**, 1688 (2005).
[3] M. Tsoi, R. E. Fontana, and S. S. P. Parkin, Appl. Phys. Lett. **83**, 2617 (2003).
[4] J. Grollier, P. Boulenc, V. Cros, A. Hamzi, A. Vaurès, A. Fert, and G. Faini, Appl. Phys. Lett. **83**, 509 (2003).
[5] C. K. Lim, T. Devolder, C. Chappert, J. Grollier, V. Cros, A. Vaurès, A. Fert, and G. Faini, Appl. Phys. Lett. **84**, 2820 (2004).
[6] S. Lepadatu and Y. B. Xu, Phys. Rev. Lett. **92**, 127201 (2004).
[7] M. Kläui, H. Ehrke, U. Rüdiger, T. Kasama, R. E. Dunin-Borkowski, D. Backes, L. J. Heyderman, C. A. F. Vaz, J. A. C. Bland, G. Faini, E. Cambril, and W. Wernsdorfer, Appl. Phys. Lett. **87**, 102509 (2005).
[8] M. Hayashi, L. Thomas, Ya. B. Bazaliy, C. Rettner, R. Moriya, X. Jiang, and S. S. P. Parkin, Phys. Rev. Lett. **96**, 197207 (2006).
[9] A. Yamaguchi, T. Ono, S. Nasu, K. Miyake, K. Mibu, and T. Shinjo, Phys. Rev. Lett. **92**, 077205 (2004).
[10] M. Kläui, P.-O. Jubert, R. Allenspach, A. Bischof, J. A. C. Bland, G. Faini, U. Rüdiger, C. A. F. Vaz, L. Vila, and C. Vouille, Phys. Rev. Lett. **95**, 026601 (2005).
[11] N. Vernier, D. A. Allwood, D. Atkinson, M. D. Cooke, and R. P, Cowburn, Europhys. Lett. **65**, 526 (2004).
[12] G. S. D. Beach, C. Knutson, C. Nistor, M. Tsoi, and J. L. Erskine, Phys. Rev. Lett. **97**, 057203 (2006).
[13] M. Donahue and D. Porter, version 1.2a3, see http://math.nist.gov/oommf/.
[14] R. D. McMichael and M. J. Donahue, IEEE Trans. Magn. **33**, 4167 (1997).
[15] M. Kläui, C. A. F. Vaz, J. A. C. Bland, and L. J. Heyderman, Appl. Phys. Lett. **85**, 5637 (2004).